This article was downloaded by:
On: *21 January 2011*
Access details: *Access Details: Free Access*
Publisher *Taylor & Francis*
Informa Ltd Registered in England and Wales Registered Number: 1072954 Registered office: Mortimer House, 37-41 Mortimer Street, London W1T 3JH, UK

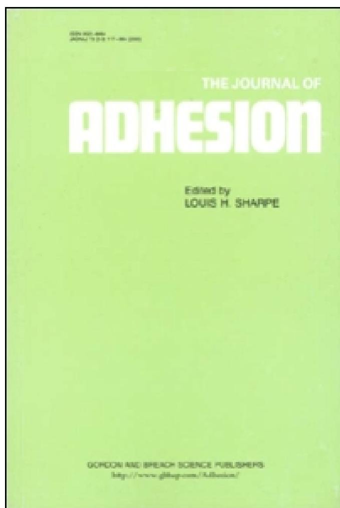

The Journal of Adhesion
Publication details, including instructions for authors and subscription information:
http://www.informaworld.com/smpp/title~content=t713453635

Force Curve Measurements with the AFM: Application to the In Situ Determination of Grafted Silicon-Wafer Surface Energies

Olivier Noel[a]; Houssein Awada[a]; Gilles Castelein[a]; Maurice Brogly[a]; Jacques Schultz[a]
[a] Institut de Chimie des Surfaces et Interfaces (ICSI-CNRS-UPR 9069), Mulhouse Cedex, France

To cite this Article Noel, Olivier , Awada, Houssein , Castelein, Gilles , Brogly, Maurice and Schultz, Jacques(2006) 'Force Curve Measurements with the AFM: Application to the In Situ Determination of Grafted Silicon-Wafer Surface Energies', The Journal of Adhesion, 82: 7, 649 — 669

To link to this Article: DOI: 10.1080/00218460600775773

URL: http://dx.doi.org/10.1080/00218460600775773

PLEASE SCROLL DOWN FOR ARTICLE

Full terms and conditions of use: http://www.informaworld.com/terms-and-conditions-of-access.pdf

This article may be used for research, teaching and private study purposes. Any substantial or systematic reproduction, re-distribution, re-selling, loan or sub-licensing, systematic supply or distribution in any form to anyone is expressly forbidden.

The publisher does not give any warranty express or implied or make any representation that the contents will be complete or accurate or up to date. The accuracy of any instructions, formulae and drug doses should be independently verified with primary sources. The publisher shall not be liable for any loss, actions, claims, proceedings, demand or costs or damages whatsoever or howsoever caused arising directly or indirectly in connection with or arising out of the use of this material.

The Journal of Adhesion, 82:649–669, 2006
Copyright © Taylor & Francis Group, LLC
ISSN: 0021-8464 print/1545-5823 online
DOI: 10.1080/00218460600775773

Taylor & Francis
Taylor & Francis Group

Force Curve Measurements with the AFM: Application to the In Situ Determination of Grafted Silicon-Wafer Surface Energies

Olivier Noel
Houssein Awada
Gilles Castelein
Maurice Brogly
Jacques Schultz
Institut de Chimie des Surfaces et Interfaces (ICSI-CNRS-UPR 9069), Mulhouse Cedex, France

Downloaded At: 20:40 21 January 2011

The atomic force microscope (AFM) can be used to perform surface force measurements in the quasi-static mode (cantilever is not oscillating) to investigate nanoscale surface properties. Nevertheless, there is still a lack of literature proposing a complete systematic and rigorous experimental procedure that enables one to obtain reproducible and significant quantitative data. This article focuses on the fundamental experimental difficulties arising when making force curve measurements with the AFM in air. On the basis of this AFM calibration procedure, quantitative assessment values were used to determine, in situ, SAM (or Self Assembled Monolayer)-tip thermodynamic work of adhesion at a local scale, which have been found to be in good agreement with quoted values. Finally, determination of surface energies of functionalised silicon wafers (as received, CH_3, OH functionalised silicon wafers) with the AFM (at a local scale) is also proposed and compared with the values obtained by wettability (at a macroscopic scale). In particular, the effect of the capillary forces is discussed.

Keywords: Adhesion; Atomic force microscopy; Calibration; Surface energy; Wetting

Received 24 October 2005; in final form 7 March 2006.
One of a collection of papers honoring Hugh R. Brown, who received *The Adhesion Society Award for Excellence in Adhesion Science*, *Sponsored by 3M*, in February 2006.
Address correspondence to Olivier Noel, Université du Maine, IUT Mesures Physiques, Avenue Olivier Messiaen, F-72085 Le Mans Cédex 9, France. E-mail: olivier.noel@univ-lemans.fr

INTRODUCTION

Nowadays, the atomic force microscope (AFM) is commonly used for investigating chemical and mechanical nanoscale surface properties [1–6]. The interest in this tool is partially due to its ability to perform accurate analysis of surface forces with a nanometer probe. Moreover, the AFM is a versatile tool, and various operating modes [7] have been developed. However, quantitative measurements are still difficult to obtain. Indeed, the calibration of the AFM is one of the most critical points in obtaining quantitative information. In general, there is also difficulty establishing a rigorous experimental procedure. Here, we focus on the calibration procedure of the AFM used to measure force curves in the quasi-static mode. In particular, we point out different fundamental aspects concerning the sources of error due to the different device components. These should be considered and minimized when doing force curve measurements. Finally, on the basis of our experimental procedure and calibration, the surface energy of rigid substrates (as received, CH_3- and OH-grafted silicon wafers) has been determined using two methods (force curve measurements on one hand and wetting experiments on the other hand). Both methods have been compared.

For the following investigations, all experimental deflection–distance curves (or DD curves) were performed in air, with a commercial apparatus (NanoscopeIIIa D3000, DD, Veeco Instruments, Secta Barbara, CA, USA) and a V-shaped nitride silicon tip.

Downloaded At: 20:40 21 January 2011

GENERAL ASPECTS

The usual commercialised AFM devices can be roughly broken up into three main independent parts (see Figure 1). The first one is the nanoscale probe made of a cantilever bearing a tip at its end. For convenient reasons, the cantilever is tilted at a 12° angle to the horizontal line. The tip radius, at the apex, is of the order of 10 nm. When interacting with the sample, the cantilever bends itself. Its deflection is then detected with an optical device consisting of a laser and a four-quadrant photodiodes detector.

In the case of the DI 3000 microscope, the probe can be vertically moved backward and forward *via* a piezoelectric ceramic (*cf*. Figure 1), while the sample remains motionless.

Force measurements with AFM in the quasi-static mode consist of recording the deflection of the spring (cantilever) while interacting with the sample surface [7,8]. Provided that the normal spring constant of the cantilever, k, is known, an interacting force, $F_{interaction}$,

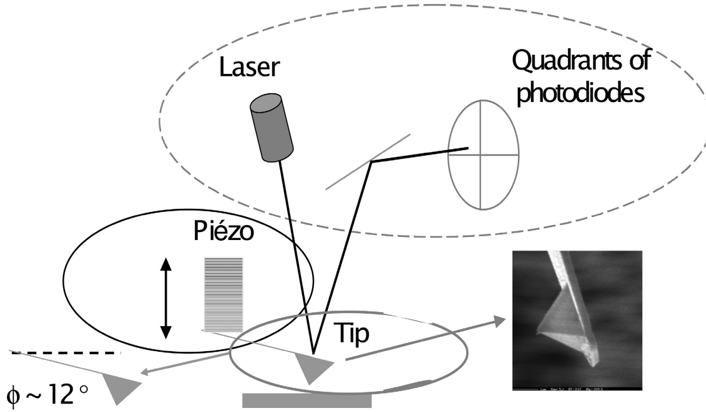

FIGURE 1 AFM schematic representation (DI 3000).

Downloaded At: 20:40 21 January 2011

can be calculated using Hooke's law:

$$F_{interaction} = -k \cdot \Delta z \quad (1)$$

where k is the cantilever stiffness and Δz is the vertical cantilever deflection.

Simultaneously, the tip is approached and retracted from the sample. Thus, it is possible to obtain DD curves and force–distance (FD) curves.

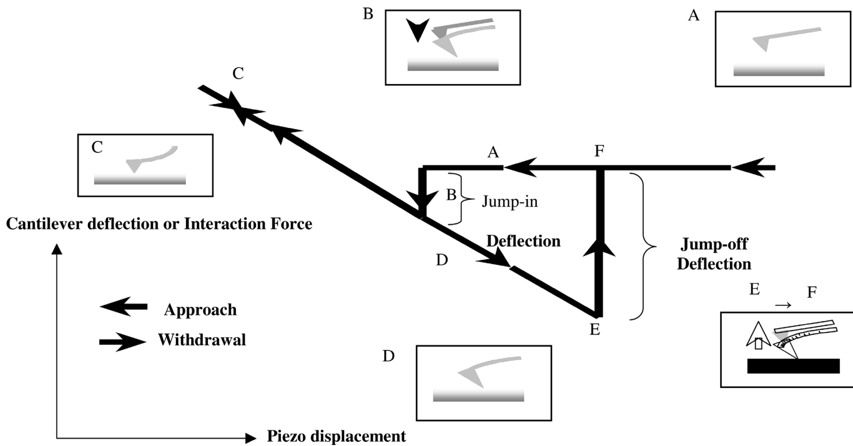

FIGURE 2 Schematic representation of a deflection–distance (DD) curve. When $k < \partial F_{interaction}/\partial D$, the tip jumps in or off the surface, because of mechanical instabilities (k is the cantilever spring constant, F the tip–sample interaction force, and D the tip–sample distance).

A schematic representation of a DD curve obtained when probing a hard surface is reported in Figure 2. In zone A, the cantilever is far from the analysed surface and stays at its equilibrium state until it jumps to the surface (zone B). When in contact (zones C and D), adhesion can be developed. Thus, during the withdrawal cycle, the jump-off (E and F) does not occur for a similar piezo displacement as for jump-in. Finally, the cantilever returns to its equilibrium state.

One should notice that jump-in observed during the approach is usually due to mechanical instabilities and is not considered here [7,8].

A prerequisite is to confirm the thermal stability of both actuator and cantilever. In our laboratory, this is achieved by switching on the AFM for at least 12 h before starting the experiments. It is also necessary to remove any external vibrational and thermal instabilities. Finally, control of the room's relative humidity is necessary [9].

Downloaded At: 20:40 21 January 2011

AFM CALIBRATION

Cantilever Calibration

According to Equation (1), it is essential to determine the cantilever stiffness, k, to obtain quantitative measurements. To achieve this goal, numerous experimental methods are described in the literature [9–19]. Each of these methods are characterised by their simplicity of implementation and precision [14,15]. We can also distinguish the destructive methods [11,16] from the nondestructive ones [14,17]. In our case, we focused on two nondestructive methods, which have been rigorously studied and compared: the first one is related to the use of rectangular reference cantilevers [19] (supplied by NanoMetrology, Nanosensors, Wetzlar, Germany) and the second is based on the thermal fluctuations measurement of the cantilever [20]. The first method is a very convenient one, as it requires only reference cantilevers and can be applied to both rectangular and V-shaped cantilevers. Moreover, the only experimental parameter to determine is the contact slope obtained on a reference cantilever and measured with the cantilever that should be calibrated. In our case, the values reported in Table 1 are an average of 10 measurements performed at the very the end of the reference cantilever and on a zone spreading on all the width of the reference cantilever. The second method requires a spectrum analyzer and the opportunity to get a raw signal (before treatment). This method consists of measuring the mean square deflection $\langle \Delta Z_c{}^2 \rangle$, due to thermal fluctuations. If the cantilever is modeled as a harmonic oscillator, the cantilever stiffness, k, is given by

TABLE 1 Cantilever Stiffness Determination, k

Thermal fluctuation method			Reference cantilever method		
Cantilever	$\langle\Delta_{z^2}\rangle(.10^{22}\ \mathrm{m}^{-1})$	k ($\mathrm{N{\cdot}m^{-1}}$)	k_{precal}	p_{percal}	k ($\mathrm{N{\cdot}m^{-1}}$)
1	1.6	0.25	0.56	0.65	0.31
2	1.3	0.30	0.56	0.66	0.30
3	1.4	0.28	0.56	0.68	0.27
4	1.5	0.27	0.56	0.65	0.31

The cantilever stiffness, k, determined by the thermal fluctuation method is given by $k = k_B T/\langle\Delta z^2\rangle$ where k_B is the Boltzmann constant, T is the temperature, and (Δz^2) is the mean square deflection of the cantilever. The cantilever stiffness, k, determined by the reference cantilevers method is given by $k = k_{precal} \times ((P_{si} - P_{precal})/(P_{precal} \times \cos\Phi))$, k_{precal} is the reference cantilever stiffness, p_{Si} and p_{precal} are respectively the slope of the force curve when the tip is respectively in contact with a silicon wafer and a reference cantilever, Φ is the cantilever tilt angle (12°).

$$k = \frac{k_B T}{\langle \Delta Z_c^2 \rangle}. \tag{2}$$

In our case, only the two first vibration modes in the spectra have been considered in the calculations [20].

In our study, five cantilevers were selected to give the same force on a reference silicon wafer. Both calibration methods have then been used and compared, to calibrate the cantilevers (*cf*. Table 1). These were triangular shaped cantilevers (supplied by Nanosensors, Wetzlar, Germany) and had an effective $0.30\,\mathrm{N \cdot m^{-1}}$ spring constant. This value is far from that specified by the supplier ($0.58\,\mathrm{N \cdot m^{-1}}$).

Tip Radius Estimation

To deduce thermodynamic parameters from experimental values, it is necessary to have a good estimation of the radius of the tip at the apex [21]. For convenient reasons, we deduced the radius on the basis of the shape revealed on a scanning electronic microscope (SEM) picture taken at the end of the measurements (Figure 3b). Both methods have given approximately the same tip radius for all used cantilevers. Our tip radius was estimated to be $50\,\mathrm{nm} \pm 5\,\mathrm{nm}$.

We have also tried to image directly the tip in AFM TappingMode$^{\mathrm{TM}}$. However, this is time consuming and not accurate (Figure 3a).

Finally, a numerical method [22] is proposed in the literature. In this method, a needle-like surface of gold (the gold is deposited by the vapor-phase deposition technique on a silicon substrate) has been used to "image" (in contact mode) the apex of the tip. Software

Downloaded At: 20:40 21 January 2011

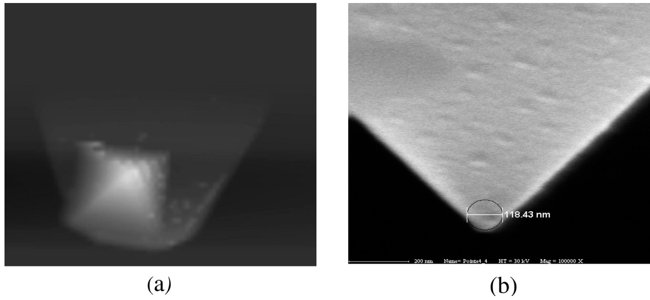

(a) (b)

FIGURE 3 Tip radius estimation (a) AFM TappingMode^{TM} imaging and (b) SEM picture.

performs a tip-reconstruction algorithm according to the technique of Villarubia [22]. Similar values of the tip radius have been obtained and compared with those from the other method.

Finally, regularly and randomly checking the adhesion force on a reference silicon wafer allows us to verify contamination of the tip or change of the tip radius during measurements. If organic tip contamination occurs, one can attempt to clean the tip by submersing it in a 2% vol. of hydrofluoric acid solution [23]. The acid solution reacts with the silicon of the tip and cleans it. After such treatment, one may recalibrate the tip.

Downloaded At: 20:40 21 January 2011

Nonlinearity of the Optical System

First of all, it is necessary to recall that this system measures the angular cantilever deflection rather than the vertical cantilever deflection. The latter is connected to the angular cantilever deflection, Δz, by a linear expression [24]. Thus, to convert the measured angular deflection into the vertical deflection, it is necessary to perform a force curve on a rigid substrate (a silicon wafer for example) and to fix the indentation slope of a force curve [or slope of the force curve in the contact zone (zones C and D in Figure 1)] to unity. However, this conversion requires two conditions to be met. The first one is that the actuator displacement is linear, and the second one is that the tip is prevented from sliding or benching on the substrate. These two conditions are discussed in the following sections.

Second, a nonlinearity of the optical detector, due to a nonhomogeneous spreading of the laser spot on the detector, was first mentioned in the literature by Haugstad and Gladfelter [25]. To study this, we have reported the indentation slope (obtained from a rigid substrate) *versus* the tension recorded by the photo detector (Figure 4). We have

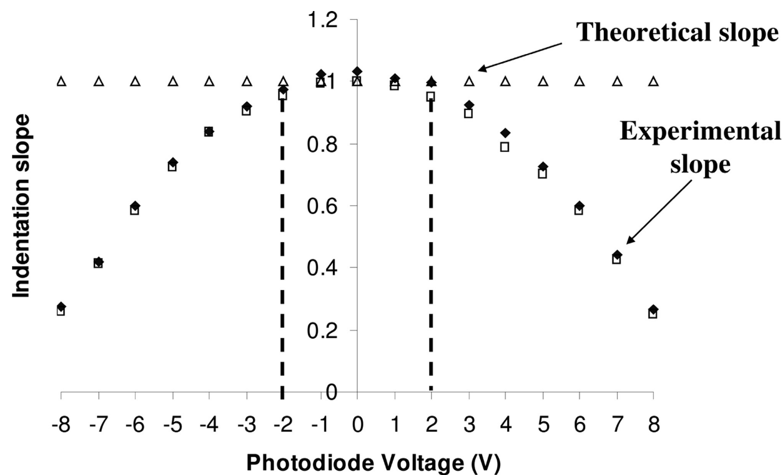

(a)

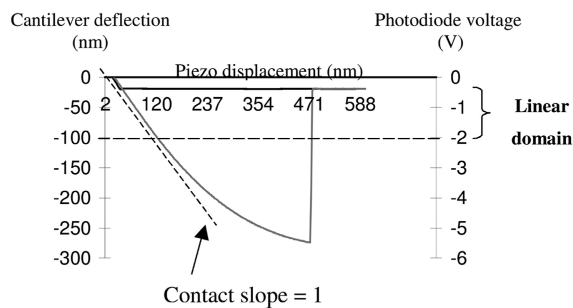

(b)

FIGURE 4 Nonlinearity of the photodetector. The two sets of experimental points (square and rhombus) represent a loading and an unloading experiment respectively.

Downloaded At: 20:40 21 January 2011

also reported the theoretical slope that is expected for a rigid substrate (its absolute value should be equal to 1). From Figure 4, we observe that the domain of linearity of the detector lies within ± 2 V. Finally, if nonlinearity is not taken into account, the error on the quantitative results can be significant. In our experiments, all the measurements have been done in the linearity domain.

Scan Speed of the Cantilever

The piezo actuator displacement is controlled by applying a voltage that lies within ± 220 V (for the NanoscopeIIIa D3000, DI). Nevertheless,

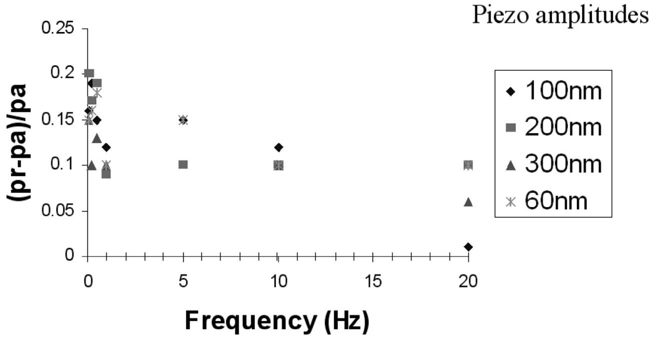

FIGURE 5 Nonlinearity of the actuator.

a linear applied tension will not generate a linear displacement. One might apply a nonlinear signal to correct it. However, this effect depends on both actuator scan speed and the total actuator displacement (piezo amplitude) and cannot be completely corrected. In addition, the actuator shows a displacement hysteresis due to the nature of the ceramic that composes the actuator. Fu [26] has shown that the piezo hysteresis can be neglected if the actuator displacement is performed around the 0 Volt applied tension. Finally, to study the nonlinearity, we have reported the relative difference of the indentation slope during loading and unloading *versus* the scan speed, for different actuator amplitudes (Figure 5). During the experiment, the actuator is considered thermally stable.

From our results, we observed that a discrepancy appears for very low scan frequencies (below 1 Hz). For higher scan frequencies (more than 20 Hz), the viscosity of the environment could be significant. It is noticeable that the dispersion of the experimental points is minimal for a 10-Hz frequency scan. Thus, this frequency is a good compromise for our actuator.

One might notice that the nonlinearity and the hysteresis of the piezo actuator are not the only parameters that could limit the scan frequencies: the sampling rate of the data has also to be taken into account.

Estimation of the Uncertainties of the Physical Values Related to the Experimental Pull-Off Force Measurements

If we consider that the main uncertainties in a pull-off force measurement using AFM are due to the determination of the spring constant and the radius of the tip, we can approximate an error of 10% for

Downloaded At: 20:40 21 January 2011

the measurement of an adhesion force (due to the uncertainty of the method of calibration of the tip, as specified by Ref. [19]), and a relative error of 20% for the determination of the work of adhesion and surface tensions (due to a 10% error on the determination of the tip radius [27]). The uncertainty of the tip radius was evaluated on the basis of nanoindentation experiments on a reference elastic polymer network. Nevertheless, even if 20% of the error is high, one must consider this error as a systematic error. Indeed, all measurements (more than 100 for a given surface) were performed with the same tip of the same radius. Experimental results are then significant, and the contribution of the different grafts can be discriminated.

WHAT DO WE REALLY MEASURE WITH THE AFM?

Effect of the Tilt Angle of the Cantilever

The previous discussion has described the main sources of error relating to the different components of the AFM and how to minimize them. Nevertheless, others problems that are directly connected to the AFM configuration have to be taken into account. In particular, one should not forget that the photodetector measures an angular cantilever deflection (θ_Z) rather than a vertical cantilever deflection (Δz) with the photodetector. Moreover, because of the tilt angle of the cantilever,

Downloaded At: 20:40 21 January 2011

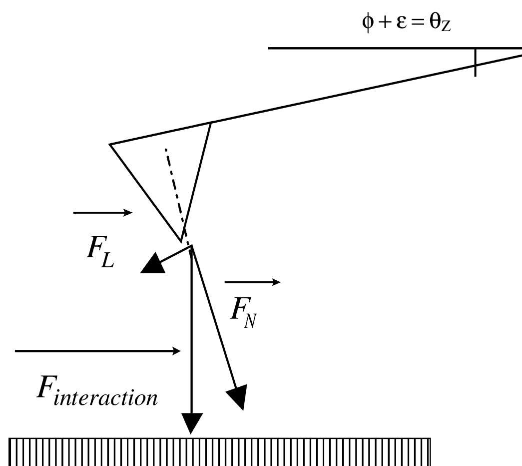

FIGURE 6 Schematic representation of the applied force on the cantilever (tilted with a ϕ angle). θ_Z is the angular cantilever deflection measured by the photo detector (ε is the angular deflection due to the interaction tip substrate).

a lateral force has to be taken into account during the measurements. Finally, the cantilever is deflected with a θ_Z angle, which can be expressed as the sum of the original cantilever tilt angle, ϕ, and the angle, ε, induced by the interaction with the sample (*cf*. Figure 6).

From this scheme, we can express the real interaction force ($F_{interaction}$) as follows (see Figure 6):

$$\overrightarrow{F_{interaction}} = \overrightarrow{F_N} + \overrightarrow{F_L}. \tag{3}$$

The normal force, F_N, induces an angular deflection of which the angle (θ_N) at the point of application of the force is given by [28]

$$\theta_N = \frac{F_N(l-b)^2}{2EI} \tag{4}$$

where b is the distance between the end of the cantilever and the point of application of the force, l is the total length of the cantilever, E is the Young's modulus, and I is the inertial moment. The lateral force (F_L) induces a moment M given by

$$M = F_L \times H \tag{5}$$

where H is the height of the tip.

This moment induces an angular deflection θ_M given by [28]

$$\theta_M = \frac{-M(l-b)}{EI}. \tag{6}$$

Finally, the angular deflection θ_Z measured by the optical detector is given by

$$\theta_z = \theta_N + \theta_M. \tag{7}$$

In conclusion, Equation (1) is true if we neglect the angular deflection due to the lateral component θ_M. For our cantilevers, the ratio θ_N/θ_M that gives the error on the vertical angular deflection is

$$\frac{\theta_M}{\theta_N} = \frac{2F_L H}{F_N l} = \frac{2\sin\phi \times H}{\cos\phi \times l} = 0.013 \tag{8}$$

where $\theta = 12^\circ, H \simeq 4\,\mu\text{m}, 1 \simeq 100\,\mu\text{m},$ and $b = 0$. We recognize a 1.3% error on the true measurement of the interaction force. This error can reasonably be neglected relative to the other and previously discussed errors. However, we should mention that this one increases when b, ϕ, or the deflection increase.

When the tip is in contact with the sample, the lateral force can have a more drastic effect on the force measurements due to sliding

Downloaded At: 20:40 21 January 2011

of the tip on the sample surface. In particular, Mazeran and Loubet [29] have shown that this effect depends on the geometry and the stiffness of the cantilever as well as on the friction coefficient of the material, whereas Warmack *et al*. [30] have observed that the lateral force represents up to 4% of the normal force contribution for a V-shaped cantilever and up to 2% for a rectangular cantilever. Moreover, they observed that the lateral forces are minimized by correctly positioning the laser beam on the cantilever. In particular, this is done for V-shaped cantilevers when the laser beam is at the free end of the cantilever.

Thus, the choice of cantilever is a compromise between obtaining high-resolution force measurements (*i.e*., a low stiffness constant cantilever) and minimizing effects of the lateral forces (*i.e*., a high stiffness constant cantilever). Additionally, one should mention that a recent study [31] has shown that a rectangular cantilever, rather than V-shaped cantilever, appears to be more appropriate for doing force curve measurements, because it minimizes the torsion effect.

Downloaded At: 20:40 21 January 2011

Effect of the Capillary Forces

For technical reasons, all the AFM measurements were done in air at about 20°C. Under these conditions, the influence of the capillary forces cannot be neglected. Indeed, all the experiments were done at a constant relative humidity of 30%. Many studies have reported the effect of humidity [9,32–36] on the pull-off force. Xiao and Qian [9] and Sedin and Rowlen [33] have shown that a water meniscus cannot be formed between the tip and the surface if relative humidity is below 20%. He and co-workers [34] have observed a meniscus formation only in the case of hydrophilic contact but not for hydrophobic contact. These results are confirmed by Zhang *et al*. [35]. Hu *et al*. [36] have observed for hydrophilic tip–mica contact that water capillary effects are significant if relative humidity is higher than 40%. As in our experiments, if the humidity is 30%, one can suspect the existence of a capillary bridge. From the theoretical point of view, the minimum thickness of the water capillary film is expressed as [37,38]

$$e = a_0\left(\frac{\gamma}{S}\right),$$

where e is film thickness, γ is surface tension of water, a_0 is capillary length, and S is spreading coefficient ($S = \gamma_S - \gamma_{SL} - \gamma_L$). As a consequence, the force measured by AFM includes the contribution of van

der Waals and capillary forces. The total adhesion force is given by the following expression:

$$F_{adhesion} = F_{cap} + F_{VdW} \tag{9}$$

The capillary force depends on a meniscus formed between the two surfaces and is given by Israelachvili [39] and by Riedo *et al*. [40], in the case of sphere–plane contact, as

$$F_{cap} = 2\pi R\gamma(\cos\theta_1 + \cos\theta_2) = 4\pi R\cos\theta, \tag{10}$$

where γ is the surface energy of the liquid ($72.6\,\mathrm{mJ\cdot m^{-2}}$ for water), θ_1 and θ_2 are the respective contact angles (of water) with the surfaces in contact (nonidentical), θ is the contact angle (of water) with the hydrophilic surface, and R is the tip radius.

Downloaded At: 20:40 21 January 2011

APPLICATION OF AFM CALIBRATION: *IN SITU* DETERMINATION OF THE SURFACE ENERGY OF RAW AND GRAFTED SILICON WAFERS

In the following, an attempt is made to determine *in situ* quantitative surface energies of different rigid substrates [as-received silicon wafer (or Si_{wafer}), CH_3 (or Si_{CH_3}), and OH (or Si_{OH}) grafted silicon wafers] on the basis of the previously described calibration procedure. In particular, pull-off force measurements were performed in ambient air. The relative humidity was maintained to a 30% level during the measurements. The stiffness of the selected cantilevers is 0.30 N/m. The scan rate is 10 Hz, and light loads were implemented to minimize probe deformation upon contact. Finally, the pull-off force was measured in the domain of linearity [−2V; 2V] of the optical detector.

In Situ Measurement of the Thermodynamic Work of Adhesion of a Silicon Wafer with the AFM

The silicon wafer was previously cleaned in hexane and then in ethanol in an ultrasonic bath. That means a contaminated layer still remains on the surface. In that case, this silicon wafer is referred as the as-received silicon wafer (or Si_{wafer}).

From the jump-off value of the force curve (in Figure 7) and Equation (1), we can deduce the adhesion force between the silicon nitride tip and the wafer of silicon ($F_{Siwafer}$). In fact, the considered adhesion force is an average adhesion force over 100 measurements for a given

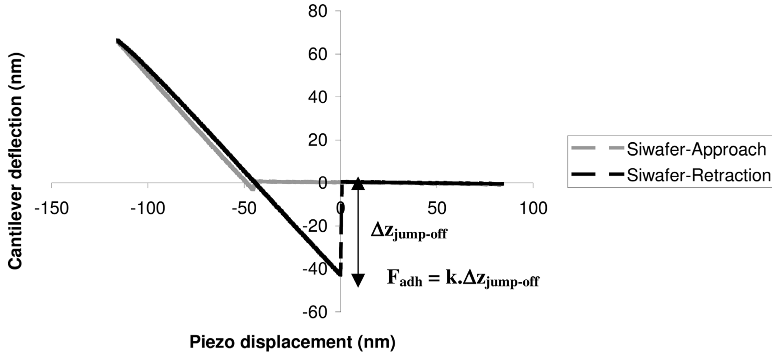

FIGURE 7 Characteristic force curve on a wafer of silicon.

surface, performed with tips that have been calibrated (same adhesion force on a reference wafer).

$$F_{Siwafer} = -k \cdot \Delta z_{jump\text{-}off} = -14.3 \pm 2\,\text{nN}. \tag{11}$$

A thermodynamic work of adhesion can be calculated from the DMT theory [41], which is suitable for rigid surfaces in contact (that is the case if we consider a nitride silicon tip in contact with a wafer of silicon):

$$W_0 = -\frac{F_{Siwafer}}{2\pi R} = 45 \pm 9\,\text{mJ} \cdot \text{m}^{-2} \tag{12}$$

where $R = 50\,\text{nm}, k = 0.30\,\text{N} \cdot \text{m}^{-1}$.

Surface Energy Determination of a Silicon Wafer

The surface free energy, γ, is related to the work of adhesion W_0 (no capillary forces are considered because Si_{wafer} is a hydrophobic surface in our case) by the following expression:

$$W_0 = \gamma_{Siwafer} + \gamma_{tip} - \gamma_{Siwafer\text{-}tip}, \tag{13}$$

where $\gamma_{Siwafer}$ and γ_{tip} are the surface free energies of the sample and the tip. $\gamma_{Siwafer\text{-}tip}$ is the interfacial tension at the tip–sample interface.

If both materials (Si_{wafer} and Si_3N_4) in contact can be approximated to be similar, then

$$\gamma_{Siwafer\text{-}tip} = 0\,\text{J} \cdot \text{m}^{-2}. \tag{14}$$

The expression of W_0 is reduced to

$$W_0 = 2 \times \gamma_{Siwafer}. \tag{15}$$

Downloaded At: 20:40 21 January 2011

On the basis of contact-angle measurements with diiodomethane and water [42] and Ref. [9], the previous hypothesis has been verified if we consider a silicon nitride tip in contact with an as-received silicon wafer. Thus, knowing W_0, we have an estimation of the surface energy ($\gamma_{Siwafer}$) of our experimental system, which is equal to $23\,mJ \cdot m^{-2}$ for the Si_{wafer}. The obtained value is in good agreement with the surface energy determined by wetting experiments [43] ($\gamma_{Siwetting} = 25\,mJ \cdot m^{-2}$).

In Situ Surface Energy Determination of a Functionalised Wafer of Silicon (CH_3 and OH Functionalised Silicon Wafers) with the AFM

In this part, we propose to determine the surface energy of two functionalised silicon wafers [Si_{CH_3} (hydrophobic surface) and Si_{OH} (hydrophilic surface)] on the basis of our AFM calibration procedure.

Functionalised Substrate Preparation

The hydrophobic surface (Si_{CH_3}) was prepared by using hexadecyltrichlorosilane ($C_{16}H_{42}O_3Si$ or Si_{CH_3}) (supplied by ABCR Karlsruhe-Germany) grafted on a silicon wafer.

Before grafting, the substrates must be chemically modified to create a hydrophilic surface (SiO_2). The silicon surface is first cleaned with ethanol and dried with nitrogen before oxidation. Then, oxidized surfaces are obtained after cleaning the substrate in a warm piranha (60°C) solution (3:7 v/v 30% H_2O_2 and H_2SO_4 mixture) for about 30 min to keep a smooth surface and then thoroughly rinsed with deionized and twice-distilled water. Just before being grafted with silane, the wafers are dried with nitrogen. This treatment produces a high hydroxyl group density on the surface (SiOH groups), to which functional silanes will adsorb upon hydrolysis.

Surfaces modified with hydroxyl groups (Si_{OH}) were synthesized with this method and immediately probed to avoid contamination of the surface by the environment due to the high reactivity of SiOH groups.

Grafting Procedure

Among numerous techniques to obtain Si_{CH_3} self-assembled monolayers (SAMs), the vapour-phase molecular self-assembling technique was used. In this method, the oxidized silica surfaces are placed above a previously de-aired solution of 100 µl of organosilane and 3 ml of paraffin mixture. The vapour-phase deposition of the molecular film on the substrate is performed in a vacuum chamber (50 min at 5×10^{-3} Torr) at room temperature.

Downloaded At: 20:40 21 January 2011

The complete experimental functionalisation procedure, as well as the surface characterisation, is described in Ref. [44]. In particular, the roughness of the functionalised surfaces has been determined with the AFM and is equal to 0.2 nm.

In Situ Surface Energy Determination of Functionalised Surfaces

Our *in situ* surface energy determination of both functionalised surfaces is based on Equation (15). Consequently, to be sure that both the surface and the tip in contact can be approximated to be similar, it is necessary to graft the AFM tip with the same terminal groups as with the analysed surfaces. To this end, we used terminated $-CH_3$ and $-OH$ function organosilanes that were grafted on a gold layer previously deposited on the nitride silicon tip. As a linkage agent between the tip and the gold, we used organic molecules such as (3-mercaptopropyl)triethoxysilane (MPS) [42]. Usually, the linkage agent for gold can be a titanium layer deposited on the tip by physical vapor deposition (PVD). However, Equation (12) shows that the thermodynamic work of adhesion is dependant on the tip radius. This tip radius is easily affected by the titanium layer deposited on the tip. In consequence, the determination of quantitative values of the thermodynamical work of adhesion can be difficult.

To check the efficiency of the linkage agent, friction experiments between a tip (covered by MPS and 10 nm of gold) and a reference surface were carried out. The experimental procedure consisted of measuring the adhesion force between the tip and the sample after a 5-min friction experiment. The same procedure is done at increasing friction-loading force to increase the force between the tip and the reference surface during friction. The adhesion force remains constant even after 60 curves. We can then deduce that the gold layer exhibits good adhesion on the tip and is not removed from the tip during friction experiments. We have also checked that the tips were not blunted during the force curve measurements by regularly measuring the adhesion force on a reference silicon wafer.

Determination of the Tip Radius

Figure 8 shows SEM pictures of $-CH_3$- and $-OH$-grafted tips with the new grafting procedure (using MPS as a linkage agent). From these pictures, we can determine a macroscopic radius of about 45–50 nm. However, one might consider that when the gold is deposited on the tip, the latter is absorbed under spherical islands. AFM images in tapping mode (Figure 9) of the gold layer, evaporated in the same conditions as the gold layer deposited on the tip, show a

Downloaded At: 20:40 21 January 2011

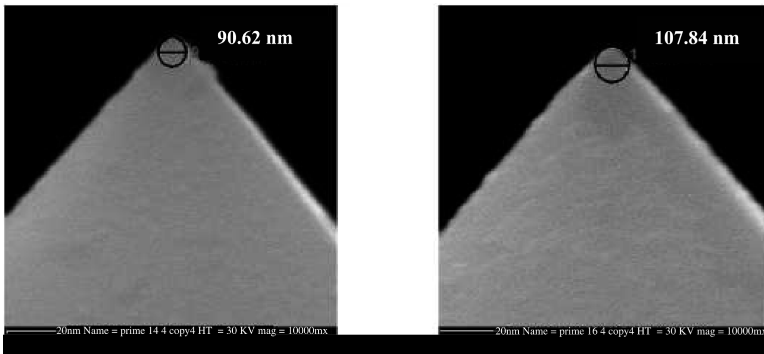

FIGURE 8 MEB pictures of grafted tips using MPS as a linkage agent between the tip and the gold layer.

Downloaded At: 20:40 21 January 2011

typical morphology of the gold aggregates. The average diameter of the islands is about 30 nm. When the tip comes into contact with the substrate, individual contacts between an island of 15 nm radius and the sample must be considered. Moreover, the section analysis of the gold layer deposited in the same experimental conditions on a flat surface proves that the height of the island is about 16 nm. The curvature of the tip imposes a contact between one island, which is located at the end of the tip, and the surface. Surface energy can then be calculated on the basis of this contact condition.

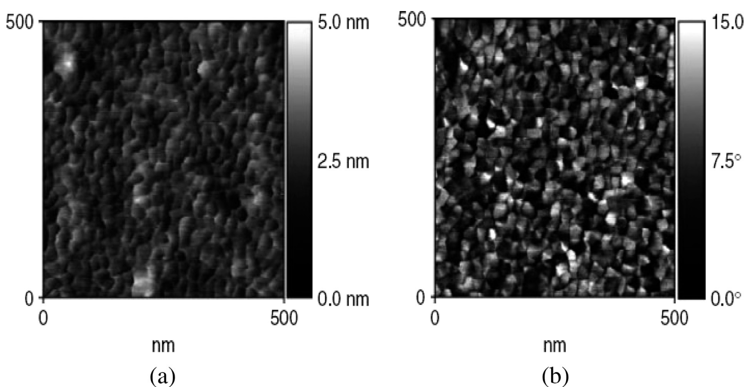

FIGURE 9 Topographic (a) and phase contrast (b) images (500×500 nm) of the gold layer deposed by PVD on reference surface, treated in the same way as the tip before grafting (silicon wafer–MPS–10-nm Au).

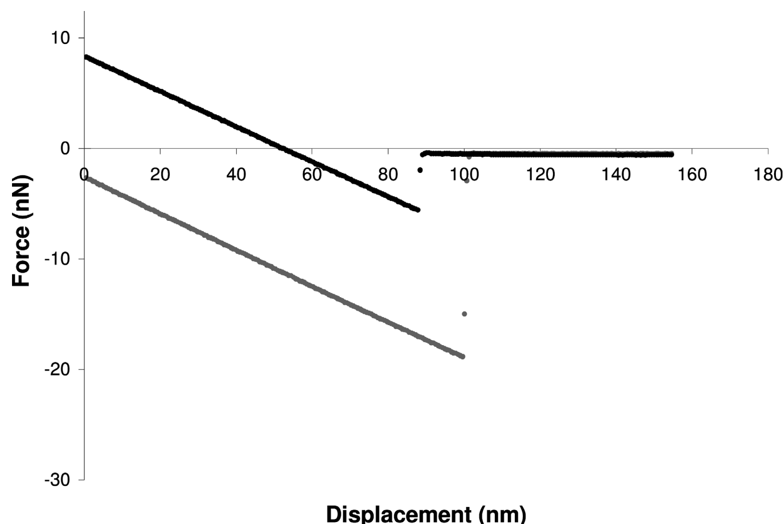

FIGURE 10 Characteristic force curve obtained with a –OH-grafted tip on a OH surface (grey curve) and a $-CH_3$-grafted tip on a CH_3 surface (black curve).

Downloaded At: 20:40 21 January 2011

Determination of the Surface Energy

Figure 10 shows the experimental curve obtained with an OH-grafted tip on an OH-grafted silicon wafer and a CH_3-grafted tip on a CH_3-grafted silicon wafer. The thermodynamic works of adhesion and the surface energies are calculated using, Equations (12) and (15) respectively. The values of the surface energies of Si_{CH_3} and Si_{OH} substrates determined by both AFM (the experimental value is an average of 120 curves) and wettability experiments are reported in Table 2. The value obtained for the Si_{CH_3} surface are in good agreement with the published value for an alkylsilane in the literature (C-18 grafting) [8,32,44,45]. The difference observed with the value

TABLE 2 Surface Energies of –OH-grafted and CH_3-Grafted Silicon Wafers and Determined Respectively, with the AFM and by Wettability Experiments

	Grafted surface	
Determination method	CH_3 (mJ/m^2)	OH (mJ/m^2)
AFM (local scale)	31 ± 6	116 ± 24
Wettability (macroscopic scale)	22 ± 2	76 ± 2

TABLE 3 Surface Energies due to the van der Waals Contributions and Determined with the AFM

	Grafted surface	
Method	CH_3 (mJ/m^2)	OH (mJ/m^2)
AFM (local scale)	31 ± 6	51.5 ± 10

obtained by wettability experiments is comprehensible. On one hand, the probe is different when comparing measurements with the AFM and by wettability. In an AFM experiment, the probe is the silicon nitride tip, whereas the probe is a water droplet in wettability. On the other hand, in the case of the hydroxylated surfaces, the −OH surface is recovered by a water layer. Thus, in a wettability experiment with water, we measure the interactions between the water drop and the water surface layer. These interactions are different from the ones due to only van der Waals interactions of the hydroxylated surface, which are measured in addition to the capillary forces by the AFM.

However, the comparison of the values of surface energies determined by both methods for the Si_{OH} surface suggests that the capillary force should contribute to a first approximation to the measured adhesion force in the case of the OH-grafted silicon wafer. The contribution of the capillary forces is calculated by Equation (10). In the case of the OH-grafted surface (the contact angle with water is $\theta = 26^\circ$ for our hydroxylated surface, and for a tip radius, $R = 15\,\text{nm}$), the capillary force F_{cap} is equal to 12.3 nN. This calculated value for the capillary force has been verified experimentally. Indeed, measurements have been done in water for the OH-tip\OH-surface system. These show that the adhesion force is lower in water (8.1 nN) compared with values obtained in the air (24 nN). Because the capillary force represents the difference between the adhesion force measured in air and in water, the value of capillary force deduced from this experiment is about 15.9 nN ($F_{cap} = 24 - 8.1\,\text{nN}$). The difference with the theoretical value of 12.3 nN can result from the differences in contact area, but the values remain in very good agreement.

In consequence, the adhesion force due only to van der Waals interactions (F_{VdW}) and determined using Equation (9) is 9.7 nN (for the SiOH substrates). Then, the surface energy due to van der Waals interactions can be recalculated from F_{VdW} using Equations (12) and (15). In Table 3, surface energy of the –OH surface due only to the van der Waals contributions is reported. This value is in agreement

Downloaded At: 20:40 21 January 2011

with the usual works of adhesion reported in the literature for organic–organic contacts (40 to 70 $mJ \cdot m^{-2}$) [47].

CONCLUSION

This study has shown that a rigorous experimental procedure and AFM calibration is necessary to get quantitative values. In particular, we have determined the cantilever stiffness, the nonlinearity of the photo detector, the nonlinearity and hysteresis of the actuator, and the effect of the tilted angle of the tip. We have observed that these parameters can drastically affect quantitative measurements. Considering that all the sources of error are minimized and controlled, we have determined quantitative surface energies of a functionalised silicon wafer that have been compared with those from wetting experiments [43]. This validates our experimental calibration procedure. Moreover, these results are original, as they are determined *in situ* with a local probe. However, quantitative measurements with an AFM are still highly questionable. In particular, the contact area (and tip shape, in general) is not easy to quantify in the case of gold coated tips [8,48] because of the roughness induced by the gold coating before grafting. To minimize this source of error, a new procedure of tip grafting with the plasma technique is still under development.

Downloaded At: 20:40 21 January 2011

ACKNOWLEDGEMENTS

The authors are grateful to P.-E. Mazeran, J.-P. Aimé, and C. Frétigny for their fruitful discussions, R. Lévy and M. Maaloum for their help with the cantilever calibration using the thermal fluctuation method, and L. Vidal for SEM pictures.

REFERENCES

[1] Leite, F. L. and Herrmann, P. S. P., *J. Adhes. Sci. Technol.* **19**, 365–405 (2005).
[2] Clear, S. C. and Nealy, P. F., *J. Colloid Interface Sci.* **213**, 238–250 (1999).
[3] Schonherr, H., Hruska, Z., and Vancso, G. I., *Macromolecules* **33**, 4532–4537 (2000).
[4] Noy, A., Vezenov, D. V., and Lieber, C., *Annu. Rev. Mater. Sci.* **27**, 381–421 (1997).
[5] Duwez, A. S., Poulenis, C., Bertrand, P., and Nysten, B., *Langmuir* **17**, 6351–6357 (2001).
[6] Noy, A., Zepeda, S., Orme, C. S., Yen, Y., and De Yoreo, J. J., *J. Am. Chem. Soc.* **125**, 1356–1362 (2003).
[7] Cappella, B. and Dietler, G., *Surf. Sci. Reports* **34**, 1–104 (1999).
[8] Butt, H. I., Cappella, B., and Kappl, M., *Surf. Sci. Reports* **59**, 1–152 (2005).
[9] Xiao, X. and Qian, L., *Langmuir* **16**, 8153–8158 (2000).
[10] Sader, J. E., Chon, J. W. M., and Mulvaney, P., *Rev. Scientific Instruments* **70**, 3967–3969 (1999).

[11] Senden, T. J. and Ducker, W. A., *Langmuir* **10**, 1003–1004 (1994).
[12] Sheiko, S. S., Moller, M., Reuvekamp, E., and Zandbergen, H. W., *Phys. Rev. B: Condensed Matter* **48**, 5675–5678 (1993).
[13] Gibson, C. T., Weeks, B. L., Abell, C., Rayment, T., and Myhra, S., *Ultramicroscopy* **97**, 113–118 (2003).
[14] Hutter, J. L. and Bechhoefer, J., *Rev. Scientific Instruments* **64**, 1868–1873 (1993).
[15] Gibson, C. T., Watson, G. S., and Myhra, S., *Nanotechnology Bristol* **7**, 259–262 (1996).
[16] Cleveland, J. P., Manne, S., Bocek, D., and Hansma, P. K., *Rev. Scientific Instruments* **64**, 403–405 (1993).
[17] Gibson, C. T., Weeks, B. L., Lee, J. R. I., Abell, C., and Rayment, T., *Rev. Scientific Instruments* **72**, 2340–2343 (2001).
[18] Notley, S. M., Biggs, S., and Craig, V. S. J., *Rev. Scientific Instruments* **74**, 4026–4032 (2003).
[19] Torii, A., Sasaki, M., Hane, K., and Okuma, S., *Measurement Scientific Technol.* **7**, 179–184 (1996).
[20] Levy, R. and Maaloum, M., *Nanotechnology Bristol* **13**, 33–37 (2002).
[21] Johnson, K. L., Kendall, K., and Roberts, A. D. *Proceedings, Royal Society* **A324**, 301–313 (1971).
[22] Villarubia, J. S., *Surf. Sci.* **321**, 287–300 (1994).
[23] Noel, O., Brogly, M., Castelein, G., and Schultz, J., *Eur. Polym. J.* **40**, 965–974 (2004).
[24] Sarid, D., *Scanning Force Microscopy with Applications to Electric, Magnetic, and Atomic Forces* (Oxford University Press, Oxford, UK, 1991).
[25] Haugstad, G. and Gladfelter, W. L., *Ultramicroscopy* **54**, 31–40 (1994).
[26] Fu, J., *Rev. Scientific instruments* **66**, 3785–3788 (1995).
[27] Noel, O., Brogly, M., Castelein, G., and Schultz, J., *MRS Proceedings* 778 (2003).
[28] Young, W. C. *Roark's Formulas for Stress and Strain* (McGraw-Hill, New York) 6th ed. pp. 98–105.
[29] Mazeran, P. and Loubet, J., *Tribology Lett.* **7**, 199–212 (1999).
[30] Warmack, R. J., Zheng, X. Y., Thundat, T., and Allison, D. P., *Rev. Scientific Instruments* **65**, 394–399 (1994).
[31] Sader, J. E. *Rev. Scientific Instruments* **74**, 2438–2443 (2003).
[32] Wood, J. and Sharma, R., *Langmuir* **10**, 2307–2310 (1994).
[33] Sedin, D. L. and Rowlen, K. L., *Anal. Chem.* **72**, 2183–2189 (2000).
[34] He, M., Szuchmacher Blum, A., Aston, D. E., Buenviaje, C., Overney, R. M., and Luginbuhl, R., *J. Chem. Phys.* **114**, 1355–1360 (2001).
[35] Zhang, L., Li, L., Chan, S., and Jiang, S., *Langmuir* **18**, 5448–5456 (2002).
[36] Hu, J., Xiao, X. D., Ogletree, D. F., and Salmeron, M., *Surf. Sci.*, **344**, 221–236 (1995).
[37] Bruinsma, R., *Macromolecules* **23**, 276–280 (1990).
[38] De Gennes, P. G., *Rev. Mod. Phys.* **57**, 827–863 (1985).
[39] Israelachvili, J., *Intermolecular and Surface Forces* (Academic Press, London, 1991), 2nd ed.
[40] Riedo, E., Levy, F., and Brune, H., *Phys. Rev. Lett.* **88**, 185505-(1–4) (2002).
[41] Derjaguin, B. V., Muller, V. M., and Toporov, Y. P. *J. Colloid Interface Sci.* **53**, 314–326 (1975).
[42] Houssein, A., Castelein, G., and Brogly, M., *Surf. Interface Anal.* **37**, 755–764 (2005).
[43] Noel, O., Brogly, M., Castelein, G., and Schultz, J., *Langmuir* **20**, 2707–2712 (2004).

Downloaded At: 20:40 21 January 2011

[44] Beach, E. R., Tormoen, G. W., and Drelich, J., *J. Adhes. Sci. Technol.* **16**, 845–868 (2002).
[45] Garth, W., Tormoen, J., Drelich, E. R., and Beach, E. R., *J. Adhes. Sci. Technol.* **18**, 1–17 (2004).
[46] Luan, B. and Robbins, M. O., *Nature* **435**, 929–932 (2005).
[47] Papirer, E., Balard, H., and Sidqi, M., *J. Colloid Interface Sci.* **159**, 238–242 (1993).

Downloaded At: 20:40 21 January 2011